Calculating the Effect of Surface or Underwater Explosions on Submerged Equipment and Structures

C. David Sulfredge, Robert H. Morris, and Robert L. Sanders
Oak Ridge National Laboratory, Building 5700, MS-6085
P.O. Box 2008, Oak Ridge, Tennessee 37831-6085

Abstract–*Since the terrorist attacks of September 11, 2001, the hazard to plant intake structures from waterborne explosives has become an area of particular concern. Both surface and underwater detonations are potential hazards to the water intakes or a plant spent fuel pool. The USS Cole incident shows the potential for terrorist attacks on our infrastructure involving waterborne bombs, yet little information on how to determine the potential damage from such scenarios is publicly available. This paper will present some techniques for calculating free-field blast parameters such as pressure and impulse in both surface and underwater explosions, as well as showing how these results can be applied to damage assessments for specific facility geometries.*

I. INTRODUCTION

In a free-field underwater detonation, the gas bubble from the explosion remains confined by water on all sides. During the initial expansion of the gas bubble after shock wave formation, the inertia of the outflowing water causes the expansion to persist until gas pressure inside the bubble drops below the corresponding hydrostatic pressure for that depth. The bubble then collapses to a high internal pressure condition and expands again. Thus the initial shock wave is followed by a further series of bubble oscillations that gradually diminish in intensity until they are damped out by viscous fluid friction. Each of these bubble oscillations transmits a secondary pressure pulse through the surrounding water. Bubble pulsation generates considerably lower peak overpressures than the primary explosion shock wave, but the time scale of the oscillations is much longer as well, so that the overall positive impulse delivered to a target may be comparable or even greater than that from the primary shock wave. The pressure and positive impulse generated by bubble oscillations vary as functions of charge weight, range, and depth. In addition, the primary shock wave intensity depends on both the charge and range and can also be affected by reflection from the bottom, other submerged structures, or the free surface of the water. Rigid surface reflections generate compression waves and free surface reflections generate rarefaction waves that superimpose on the original shock waveform. This paper describes some methods that allow all these free-field blast parameters for underwater explosions to be estimated by scaling from available experimental data, including the effects of surface and bottom reflection.

For a surface explosion the gas bubble from the charge immediately vents to the atmosphere, so there are no subsequent bubble oscillation pressure pulses. Thus the shock wave is the primary energy transmission mechanism through the water, and reflection of the shock wave from the free surface is not a major concern. There is also a substantial attenuation of both pressure and positive impulse compared to an explosion completely surrounded by water. Much less data are available for the case of surface explosions than for completely submerged bursts, but it is still possible to estimate both free-field shock overpressure and impulse as functions of range and depth.

The objective for analyzing the surface explosion of a waterborne boat bomb is to determine the peak shock wave pressure and shock wave positive impulse as functions of target depth and radial distance from the detonation point. Calculated parameters needed for the underwater blasts include peak pressure and total positive impulse for both the shock wave and bubble oscillation phases of the explosions. These parameters need to be determined as functions of range and charge depth extending out into the surrounding water from a position immediately adjacent to the explosion.

II. SURFACE EXPLOSION PARAMETERS

As discussed in the Introduction, a surface blast allows almost instantaneous venting of the gas bubble to the atmosphere. Thus bubble oscillations do not occur, and shock wave parameters are the primary concern. Peak shock wave pressure for these cases can be obtained from an NSWC report by Swisdak (Ref. 1), where the data for peak pressure is presented in the nomograph reproduced in Fig. 1 as functions of charge weight, target depth, and radial distance. When the data range available in the nomograph is insufficient, correlations from R. H. Cole's book on underwater explosions (Ref. 2) and data from Russian hydroacoustic experiments in a shallow reservoir (Refs. 3-4) can be used to extrapolate as necessary in terms of radial distance. No basis is available to extrapolate the Swisdak data beyond the specified range of target depths. However except at the shallowest depths, peak shock wave pressure from surface explosions increases only weakly with target depth. Hence the surface explosion parameters for each charge weight are assumed to be constant on the remainder of the range from the greatest target depth in the Swisdak data down to 100 ft.

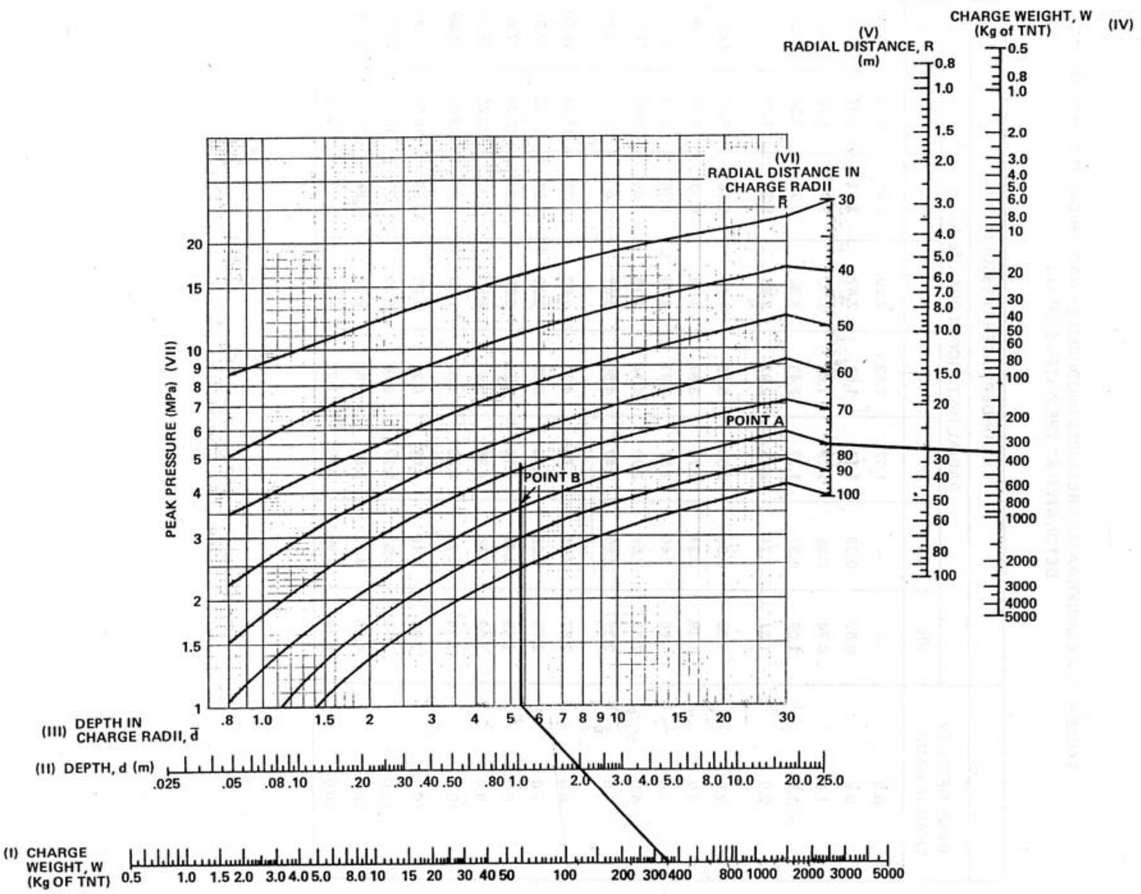

Fig. 1. Experimental data obtained by Swisdak (Ref. 1) on peak overpressure from surface explosions.

According to Cole's correlations (Ref. 2) for free-field underwater TNT explosions, the peak shock wave pressure (in psi) and integrated impulse per unit area (in psi•s) are given by:

$$P_m = 2.16 \times 10^4 \, (W^{1/3}/R)^{1.13} \qquad (1)$$

$$I/A = 1.46 \, W^{0.63}/R^{0.89} \qquad (2)$$

where W is the charge weight in pounds and R is the range in feet. Therefore, for a given charge weight the peak shock wave pressure would be expected to vary as $(1/R)^{1.13}$. Surface explosions actually experience a somewhat greater attenuation with distance than this because of energy losses to the atmosphere and rarefaction waves reflected from the free surface of the water. In some of the Russian hydroacoustic experiments reported by Eneva, et al., (Refs. 3-4) 100-kg TNT charges were fired on the surface and at various depths in a 3-m deep reservoir. Complete pressure-time histories for these tests at several ranges from the charge are reproduced in the referenced publications. Based on comparison of the waveforms at distances of 15 m and 30 m from a surface burst, the peak pressures are attenuated by an additional factor of 0.6–0.8 beyond the normal scaling effect of $(1/2)^{1.13} = 0.457$ when going from 15 m to 30 m from the charge. An average surface attenuation factor of 0.7 is assumed for any doubling of the radial range when extrapolations were needed from the Swisdak nomograph.

Swisdak did not include any data for the positive impulse associated with surface blasts in his report. However, it is possible to estimate this information by using his peak pressure results together with Cole's correlations and Eneva's Russian database. Comparing Eneva's pressure-time histories for surface vs submerged explosions (Refs. 3-4) shows that in such situations the shape and duration of the waveform are little affected by surface attenuation. Instead only the amplitude of the pulse tends to be reduced by an approximately constant factor. Since the positive impulse delivered to a target is simply the time integral of this waveform, it follows that the surface attenuation coefficient can be factored outside the integral. This then reduces the remaining integral to an impulse based on free-field pressure-time histories that can be evaluated from Cole's correlation in Eq. (2). Thus once peak shock wave pressure is available for a surface blast case by evaluating or extrapolating $P_{m,\ Swisdak}$ from the Swisdak nomograph, the corresponding positive impulse can be calculated. First, Cole's correlations for free-field blast parameters in Eqs. (1) and (2) must be evaluated for the same range and charge weight to determine $P_{m,\ Cole}$ and $(I/A)_{Cole}$. The shock wave positive impulse for the surface blast is then obtained from

$$I/A = (I/A)_{Cole}\,(P_{m,\ Swisdak}/\ P_{m,\ Cole}) \qquad (3)$$

To illustrate the surface blast effects parameters that can be calculated using these methods, Table I presents the peak shock overpressures and positive impulses expected at various depths and radial ranges from the surface detonation of a 1000-lb TNT charge. Analogous

TABLE I
Surface Blast Effects for W = 1000 lbs TNT Equivalent

Depth (ft)	Range (ft)	Peak Shock Wave Pressure (psi)	Shock Wave Positive Impulse (psi•s)
0	25	2811	2.367
	50	899	0.894
	75	450	0.493
	100	189	0.222
10	25	6350	5.348
	50	2031	2.02
	75	1131	1.24
	100	689	0.809
20	25	7710	6.493
	50	2466	2.453
	75	1378	1.511
	100	812	0.954
30	25	8163	6.875
	50	2611	2.597
	75	1523	1.67
	100	899	1.056
40-100	25	8617	7.257
	50	2756	2.741
	75	1595	1.749
	100	943	1.108

results are also shown graphically in Figs. 2-3. As an example of the calculation procedure, the peak shock overpressure of 899 psi at a range of 50 ft and zero depth was read directly from the Swisdak nomograph in Fig. 1. Evaluating Cole's free-field peak pressure and impulse per unit area correlations (Eqs. 2-3) for this charge weight and range yields $P_{m,\ Cole} = 3504$ psi and $(I/A)_{Cole} = 3.4855$ psi•s. Therefore:

$I/A = 3.4855(899/3504) = 0.894$ psi•s as reported

Although the 25-ft range at zero depth is off-scale on the nomograph, extrapolation from the 899 psi value at 50-ft range is possible based on the $(1/R)^{1.13}$ dependence from Eq. (1) and the average surface attenuation factor of 0.7 expected for a doubling of the range. Thus at a range of 25 ft:

$P_m = 899\ (2)^{1.13}/0.7 = 2811$ psi as in Table I.

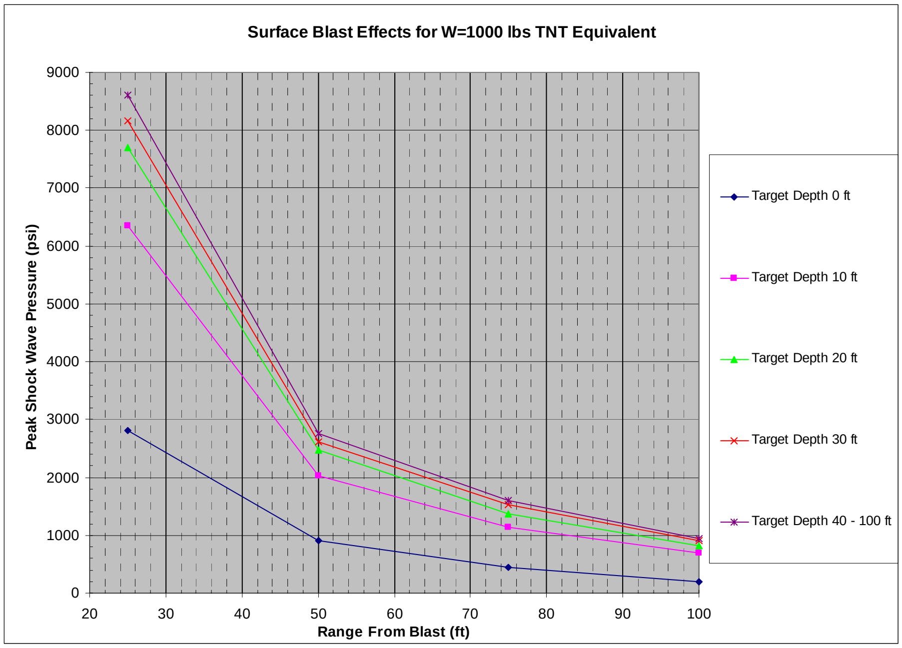

Fig. 2. Peak shock wave pressures for 1000-lb TNT surface blast.

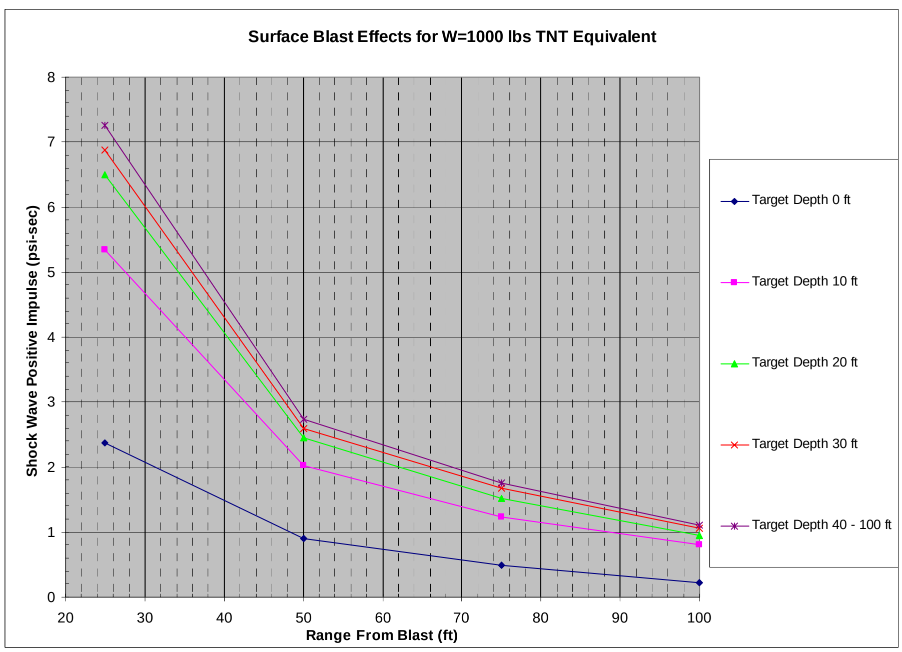

Fig. 3. Shock wave positive impulse for 1000-lb TNT surface blast.

III. UNDERWATER EXPLOSION PARAMETERS

For an underwater explosion, the gas bubble formed by the charge ordinarily does not vent immediately to the atmosphere, so that bubble oscillations are a potential source of secondary pressure pulses. Therefore for each combination of charge weight and depth, four things need to be determined: Shock wave peak pressure, shock wave positive impulse, bubble pulse peak pressure, and bubble pulse positive impulse. Robert Cole's book *Underwater Explosions* (Ref. 2) includes some very useful experimental data for these parameters based on testing of 300-lb TNT charges in about 100 ft of water. These results are summarized in Table II. They clearly show the enhancement of the shock wave parameters that occurs when a charge is fired directly on the bottom and the increased bubble pulse pressures present at around 20-ft depth for charges of this size. The latter anomaly may be due to air from the atmosphere being sucked into the gas bubble during its initial expansion (which enhances the chemical reactions and energy release during subsequent compressions), but a completely satisfactory explanation is currently not available for this experimentally observed phenomenon.

TABLE II
Shock Wave and Bubble Pulse Pressures and Impulse Data for R = 60 ft from 300-lb TNT Charges in about 100 ft of Water (Ref. 2)

	Charge depth (ft)	Peak pressure (psi)	Positive impulse (psi•s)
Shock wave	40	1770	1.15
	Bottom	1940	1.41
Bubble pulse	20	428	1.1
	26	71	0.84
	45	56	1.5
	65	84	4.0
	96	81	1.2

The data in Table II are based on a standoff distance of 60 ft and include the effects of both bottom reflection (leading to an increase in the total superimposed overpressure and impulse) and surface rarefaction cut-off (the rapid drop in overpressure associated with arrival of the rarefaction wave reflected from the free surface of the water). These tests are particularly well suited for use in assessing the threat to water intake facilities because the TNT charge weight and water depth are both in the specific range of interest.

The functional relationships needed to scale from this data are also available in Cole (Ref. 2):

Peak shock pressure varies as $(W^{1/3}/R)^{1.13}$
Peak bubble pulse pressure varies as $W^{1/3}/R$
Shock wave positive impulse varies as $W^{0.63}/R^{0.89}$
Bubble pulse positive impulse varies as $W^{2/3}/R$

As an example of how Cole's underwater explosion data from Table II can be scaled to other charge weights, depths, and ranges using these functional relationships, Table III gives the corresponding results for 100-lbs of TNT at a radial standoff range of 15 ft and depths from 5 to 100 ft. Figures 4-5 present the same information in graphical form. Generation of these results from the experimental data is a quite straightforward scaling procedure. For instance the shock wave peak pressure and impulse at 40-ft depth are obtained as follows:

Peak shock wave pressure = $1770 \times (100/300)^{1.13/3}(60/15)^{1.13} = 5605$ psi
Peak shock wave positive impulse = $1.15 \times (100/300)^{0.63}(60/15)^{0.89} = 1.98$ psi•s

And for the bubble pulse parameters at 45-ft depth:

Peak bubble pulse pressure = $56 \times (100/300)^{1/3}(60/15) = 155$ psi
Bubble pulse positive impulse = $1.5 \times (100/300)^{2/3}(60/15) = 2.87$ psi•s

Predictions for other charge weights and ranges can be developed in the same manner.

TABLE III

Underwater Blast Effects for W= 100 lbs TNT Equivalent
Standoff Distance = 15 ft Gas Bubble Radius

Charge Depth (ft)	Peak Shock Wave Pressure (psi)	Peak Bubble Pulse Pressure (psi)	Shock Wave Positive Impulse (psi•s)	Bubble Pulse Positive Impulse (psi•s)
5	5605	1187	1.98	2.11
10	5605	1187	1.98	2.11
15	5605	1187	1.98	2.11
20	5605	1187	1.98	2.11
25	5605	362	1.98	1.69
30	5605	188	1.98	1.88
35	5605	177	1.98	2.21
40	5605	166	1.98	2.54
45	5605	155	1.98	2.87
50	5605	175	1.98	4.07
55	5605	194	1.98	5.27
60	5605	214	1.98	6.46
65	5605	233	1.98	7.66
70	5605	232	1.98	6.8
75	5605	230	1.98	5.93
80	5605	229	1.98	5.07
85	5605	228	1.98	4.2
90	5605	227	1.98	3.34
95	5605	225	1.98	2.47
100	6143	225	2.42	2.3

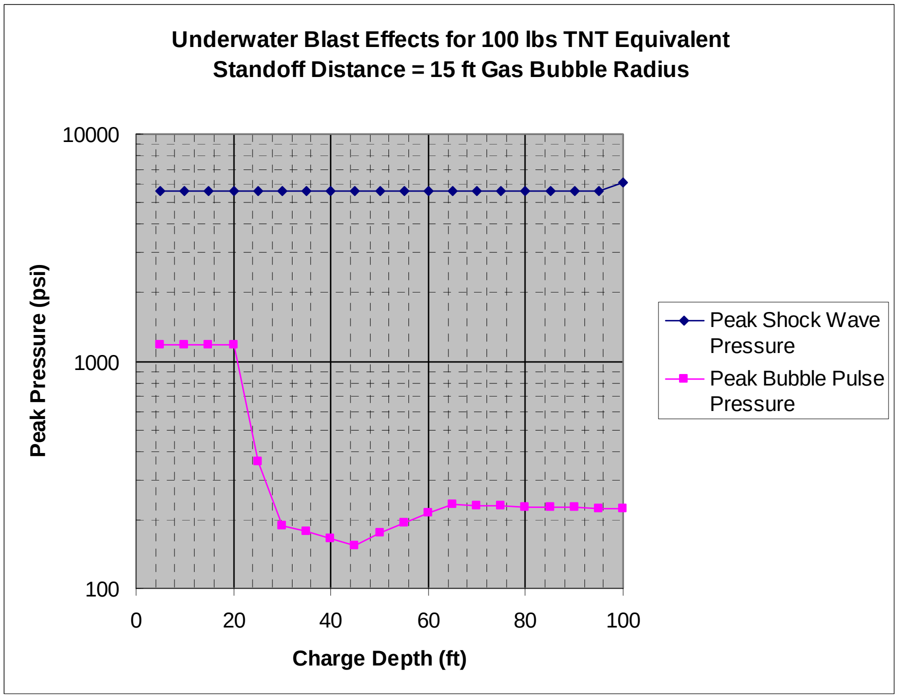

Fig. 4. Peak pressures for 100-lb TNT underwater explosion.

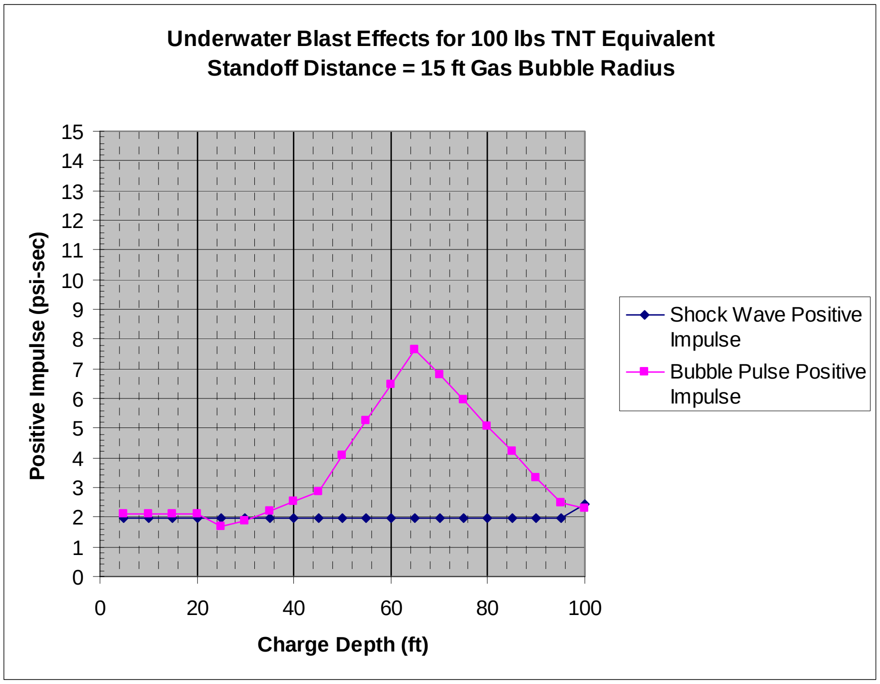

Fig. 5. Positive impulses for 100-lb TNT underwater explosion.

Linear interpolation is used to fit in for charge depths between the existing Cole data points, and enhancement of the shock wave for a charge fired on the bottom is only included for the 100-ft charge depth. All blast parameters were calculated at a distance from the charge of R = 15 ft which is equal to the radius of the gas bubble formed by the blast. The relevant average gas bubble radii are obtained from NDRC experimental data given in White, et al., (Ref. 5) and range from 10 ft up to 25 ft depending on charge size for underwater detonations of 25 lbs up to 500 lbs of TNT equivalent. At ranges less than the gas bubble radius, direct contact would occur between the gas bubble and the target rather than pressure propagation through the water. The results for predicted peak pressure and positive impulse would not apply under those conditions.

IV. EXPLOSIONS INTERNAL TO A STRUCTURE

Structural responses such as acceleration and strain levels from surface or underwater explosions are influenced by a number of considerations. Depending on their rigidity, inertia, and static strength, targets may be primarily sensitive to either peak overpressure, positive impulse, a combination of the two, or some particular aspect of their structural response such as peak translational velocity, displacement, or acceleration. If the time scale of the pressure pulses is short relative to the natural frequency of the target, as is typical of massive rigid structures, total integrated impulse delivered to the target is the primary damage mechanism. With less rigid structures that displace easily, the peak overpressure experienced by the target is a better indicator of damage. Either the primary shock wave or the bubble oscillation phase may be the dominant regime for causing damage under different circumstances. Reflective enhancement of the shock wave by the structure itself may also be a factor to consider. This paper provides some guidelines for determining which blast phenomena are most significant for particular cases and how to scale them from the available test data. The methodology developed should be valuable for conducting vulnerability assessments on a wide variety of structures, including spent fuel pools, submerged pipelines, and water treatment facilities.

When an underwater shock wave propagates into a plant intake facility, it will impact on the service water and circulating water pump inlet pipes/impellers as well as the concrete structure of the facility itself. The authors of this paper believe the most likely failure mode that could obstruct delivery of water to the plant would be crushing of the inlet pipes to the circulating or service water pumps, or explosive deformation of the piping that would bind a pump impeller. It is believed that damage to the concrete structure is not likely to interrupt water flow except for blasts large enough to have already affected the piping or impellers as well. Thus the analysis done for specific plants in this paper will focus on potential blast scenarios to damage the circulating or service water pump equipment in an intake structure.

IV.A. Plant Intake Structure Analysis

An elevation drawing of a plant intake structure is shown in Fig. 6, and a plan view is presented in Fig. 7. For this structure, the objective was to estimate the peak pressure and total positive impulse delivered to the service water or circulating water pump equipment and the potential for damage to this equipment from underwater detonations inside the structure. Various charge weights and positions were considered. Reflective enhancement of the peak pressure and impulse was included in the calculations by invoking the acoustic approximation and waveform superposition techniques described by Cole (Ref. 2). Damage to the concrete structure of the intake facility will not be analyzed.

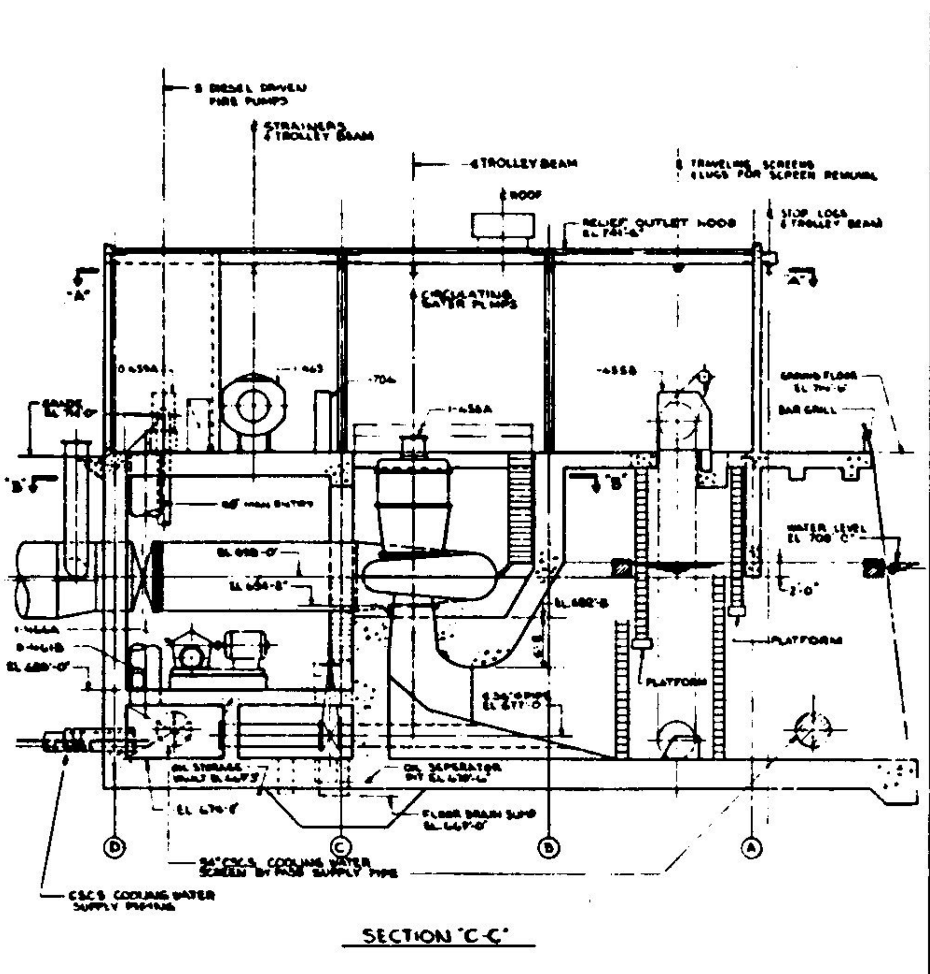

Fig. 6. Elevation view of a plant intake structure.

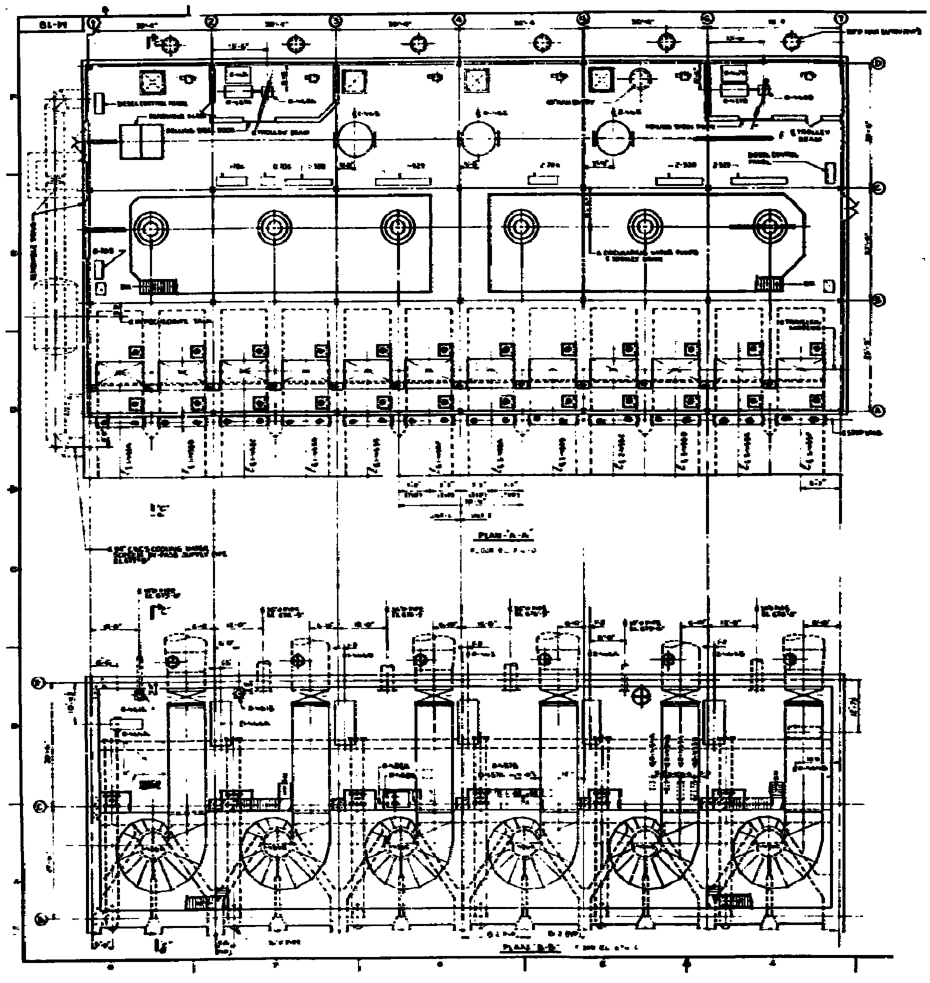

Fig. 7. Plan view of a plant intake structure.

The first charge to be considered will be 25 lbs of TNT equivalent centered at the front of the intake structure. A sketch indicating this position can be seen in Fig. 8 with the blast point marked by an asterisk. From the blast point, the circulating water pumps are located 54.0 ft back into the intake structure, and the safety-related service water pumps are behind them at a distance of 83.3 ft from the explosion. Normal water depth at the front of the intake structure is about 25.5 ft, which is only a bit more than twice the 10 ft gas bubble radius from a 25-lb charge. Under these conditions, venting is rapid enough that bubble oscillatory behavior is not much of a factor, so analysis focused on shock wave pressure and impulse. Also, in water this shallow the positive shock wave reflected vertically off the bottom and the rarefaction wave reflected vertically from the free surface would largely offset one another, leaving the horizontal shock reflections from the structure to be analyzed.

According to the acoustic approximation, each rigid reflecting surface gives rise to a reflected shock wave that appears to originate from a mirror image of the blast point behind the reflecting surface. Some of these images are denoted by circled asterisks in Fig. 8. The pressure-time history at any point is then given by the superposition of the initial and all reflected shock waves. The acoustic reflection model is strictly true only in the case of perfectly rigid reflective surfaces and moderately strong shocks, but it is a good approximation that usually gives conservatively high blast parameters because some energy is always lost during reflection (Refs. 2 and 5).

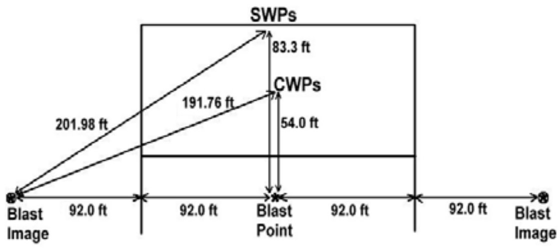

Fig. 8. Sketch showing the first blast point relative to the pump intake locations.

The reflective walls themselves would expect to see a doubling of the free-field peak pressure and impulse during reflection. Since the time-integral of a superposition sum is equal to the sum of the integrals for the individual waves, it follows that the total impulse delivered at any point in the pressure field is simply the sum of the impulses from each individual primary or reflected wave treated as a free-field calculation. The peak shock wave pressure of the superimposed wave is not equal to the sum of the peak pressures for its components unless the component time-histories are in phase with one another so that their peaks arrive simultaneously. Otherwise, a complicated waveform with several peaks will result as the peak of one shock wave is superimposed on the tail of another.

To calculate the blast conditions, it is necessary to use the methods from Sect. III to find the underwater explosion parameters for 25 lbs of TNT at all the ranges defined by Fig. 8. These results are given in Table IV.

TABLE IV
Underwater Explosion Parameters for 25-lbs TNT Equivalent at Specified Ranges

Range (ft)	Peak pressure (psi)	Positive impulse (psi•s)
54	782	0.264
83.3	479	0.180
92	428	0.164
191.76	187	0.0855
201.98	176	0.0816

These values allow calculation of the superposition for both peak pressure and impulse at the service water and circulating water pump locations. The drawings show that each set of pumps has an additional reflective surface immediately behind it (for which the mirror image point is not shown in Fig. 8 to keep the figure from becoming too cluttered). Hence the circulating pumps would be subjected to a primary and a reflected shock wave from 54.0 ft and 2 reflected waves (one from each side of the intake structure) at a distance of 191.76 ft. The superposition of these waves is then

At the circulating water pump location:

$I/A = 2(0.264) + 2(0.0855) = 0.699$ psi•s
$P_m = 2(782) = 1564$ psi, with a secondary peak of at least $2(187) = 374$ psi arriving later.

Similarly, the service water pumps would be subjected to a primary and a reflected shock (in phase with each other) from a distance of 83.3 ft and later 2 reflected waves (also in phase with each other) from a distance of 201.98 ft.

At the service water pump location:

$I/A = 2(0.180) + 2(0.0816) = 0.5232$ psi•s
$P_m = 2(479) = 958$ psi, with a secondary peak of at least $2(176) = 352$ psi arriving later.

The peak pressure and impulse on the sides of the structure during the reflection would be about $2(428) = 856$ psi and $2(0.164) = 0.328$ psi•s.

If the charge weight is increased to 100-lbs of TNT equivalent in the same position, the relevant pressures and impulses are as shown in Table V.

TABLE V
Underwater Explosion Parameters for 100-lbs TNT Equivalent at Specified Ranges

Range (ft)	Peak pressure (psi)	Positive impulse (psi•s)
54	1318	0.632
83.3	808	0.430
92	722	0.394
191.76	315	0.205
201.98	297	0.196

Now at the circulating water pump location:

$I/A = 2(0.632) + 2(0.205) = 1.674$ psi•s
$P_m = 2(1318) = 2636$ psi, with a secondary peak of at least $2(315) = 630$ psi arriving later.

And at the service water pump location:

I/A = 2(0.430) + 2(0.196) = 1.252 psi•s
P_m = 2(808) = 1616 psi, with a secondary peak of at least 2(297) = 594 psi arriving later.

The peak pressure and impulse on the sides of the structure during the reflection would be about 2(722) = 1444 psi and 2(0.394) = 0.788 psi•s.

If the 100-lb charge is fired off center and facing directly into one of the 2 main bays of the intake structure, one would have the new schematic from Fig. 9 and need some additional range parameters as given in Table VI.

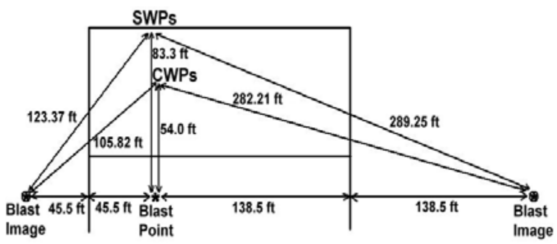

Fig. 9. Sketch showing an off-center blast point relative to the pump intake locations.

TABLE VI
Additional Underwater Explosion Parameters for 100-lbs TNT Equivalent at Specified Ranges

Range (ft)	Peak pressure (psi)	Positive impulse (psi•s)
45.5	1600	0.763
105.82	616	0.347
123.37	518	0.303
138.5	455	0.273
282.21	203	0.145
289.25	198	0.142

This configuration means that the reflected shock waves from the 2 sides of the intake structure are no longer equal in magnitude or synchronized in phase.

Now at the circulating water pump location:

I/A = 2(0.632) + 0.347 + 0.145 = 1.756 psi•s
P_m = 2(1318) = 2636 psi, with subsequent pulses of at least 616 psi and 203 psi.

And at the service water pump location:

I/A = 2(0.430) + 0.303 + 0.142 = 1.305 psi•s
P_m = 2(808) = 1616 psi, with subsequent pulses of at least 518 psi and 198 psi.

These values are slightly higher than for the centered 100-lb charge. The peak pressure and impulse on the near wall during reflection would be 2(1600) = 3200 psi and 2(0.763) = 1.526 psi•s. Corresponding values for the far wall are 2(455) = 910 psi and 2(0.273) = 0.546 psi•s.

If the charge is moved further back into the intake structure near the traveling screens, the free surface reflection likely would be eliminated because the explosion would take place below a concrete slab at elevation 607.5 ft. This change would potentially increase the delivered impulse by another factor of 4, in addition to some further enhancement resulting from the reduction in standoff from the pumps. There would also be some enhancement in the peak pressure P_m, which would depend on the precise timing of the reflected shock pulses. In addition, bubble oscillation pressure pulses could become a factor because immediate venting of the gas bubble to the atmosphere would be inhibited this far inside the structure.

For charges of W = 250 lbs, the gas bubble formed by the blast has a radius of approximately 20 ft, and for W = 500 lbs the radius is above 25 ft. Pressures inside the gas bubble are high enough that any pumps or intake piping within the bubble is likely to be destroyed or rendered unusable. A gas bubble 40-50 ft in diameter would encompass a large fraction of the space inside the intake structure. However, it should be noted that the gas bubble from even a 25-lb charge can approach 20 ft in diameter and would do substantial damage to anything directly in contact with it.

The overall blast fragility of any system also depends on many factors that have not been considered in the preceding analysis. However even relatively small charges can clearly generate significant pressure and impulse loadings if they are allowed to penetrate inside the intake structure. For this structure design, the service water pumps that provide water to safety-related systems are located behind the non-safety related circulating water pumps. This arrangement does improve intake structure security somewhat. Still, it is important to keep waterborne charges from entering the intake structure if at all possible.

IV.B. Spent Fuel Pool Analysis

Another possible application of these analysis techniques involves an explosion in a spent fuel pool and the blast environment that might result. One particularly interesting question concerns the dampening effect of the spent fuel assemblies in the pool on the explosion shock wave. Damaging those assemblies near the detonation point would absorb energy from the blast wave, reducing the pressure propagated into the remainder of the pool compared to the case where no assemblies were present. Unfortunately, very few experimental investigations of this situation have ever been carried out.

Some data is available from a ¼-scale experiment conducted in January 1997 involving the explosion of a bomb in a spent fuel pool holding canned Magnox-reactor type fuel (Ref. 6). A photograph of the experimental setup is presented in Fig. 10, showing the 400 scaled canisters stacked in the bottom of the pool with pressure gauges mounted on the pool walls. After the photograph was taken, the pool was filled with water and a scaled charge consisting of 3 lbs of C4 was detonated in the opening at the center of the canister array. Standoff distances between the burst point and the pressure sensors were about 40 inches to the gauge on the east wall of the test structure and 30 inches to the gauge on the closer south wall. The experimental report (Ref. 6) for this scaled test includes complete pressure traces as functions of time for both gauges. The peak pressures observed were about 4100 psi on the east wall gauge and 5000 psi on the south gauge.

Fig. 10. Experimental setup for spent fuel pool blast test.

Using the formula from Eq. (1) with a TNT equivalence for C4 of 1.4 and assuming full acoustic reflection of the shock waves at the pool walls as in Sect. IV.A, the predicted gauge readings are:

$P_m = 2\ (2.16 \times 10^4)\ [(3 \bullet 1.4)^{1/3}/(40/12)]^{1.13} =$ 19028 psi on the east wall

and

$P_m = 2\ (2.16 \times 10^4)\ [(3 \bullet 1.4)^{1/3}/(30/12)]^{1.13} =$ 26337 psi on the south wall

Thus the peak pressure attenuation ratios are given by:

East wall attenuation ratio = (4100 psi)/(19028 psi) = 21.55 %
South wall attenuation ratio = (5000 psi)/(26337 psi) = 18.98 %

Hence the presence of the simulated spent fuel canisters (and the shallow character of the pool) led to an approximately 80% reduction in the peak shock pressure in the pool following the explosion. Due to the rapid pressure venting in a spent fuel pool blast scenario, bubble oscillation pressure pulses would not be a significant factor influencing the blast environment.

V. CONCLUSIONS

The potential range of surface or underwater explosions can be subdivided into a number of cases (close or far-field and confined or unconfined), and in only some of these situations is the ORNL data in this paper applicable. For far-field, unconfined cases (either surface or underwater), the peak pressure and integrated positive impulse results generated by ORNL can be used as inputs for the vulnerability assessment of a structure. Cases involving confined blasts where a structure is not in close proximity to the charge can be treated using superposition calculations based on the waveforms from the reference *Underwater Explosions* by R. H. Cole (Ref. 2). For cases where conditions very close to the blast are of interest, analysis would probably require the use of hydrocodes like CTH or DYNA-3D. In contact explosions like these, the detonation of TNT converts the explosive to product gases at approximately 3000°C and a pressure of about 50,000 atm (735,000 psi). Pressures of this magnitude are cited in both Cole (Ref. 2) and Robinson (Ref. 7). Cole also indicates that the initial shock wave entering the water at the surface of the charge can have a pressure of 2,000,000 psi and that a 300-lb TNT charge with a gas bubble radius of above 20 ft would have a shock overpressure of 34,000 psi within the gas bubble at R = 5 ft. Based on these pressure results (which are far beyond the mechanical strength of materials), any equipment or structures within the gas bubble formed by the explosion would be at risk for damage. Detailed analysis would be necessary to determine the final damage state in such a contact explosion situation.

Surface boat explosions are relatively easy to analyze without the use of hydrocodes because bubble oscillations and surface reflections are not usually factors and the structure design itself typically guarantees a reasonable standoff distance to vital equipment. Furthermore, additional barriers located at modest distances from the structure can provide security against relatively large charges. Underwater explosions within an intake structure are more difficult to analyze due to multiple reflective effects and the potential for direct interaction between the gas bubble and important structures or equipment. All these effects are highly dependent on the specific geometry and charge configuration involved. Precise understanding of such a specific case would require hydrocode modeling and probably some scaled testing as well. However, the calculations documented in this report show that even relatively small charges have the potential to do serious damage if they are allowed to penetrate inside an intake structure. Care should be taken not to let this situation arise.

Predicting the degree of uncertainty in the surface and underwater explosion parameters is difficult because of the limited amount of experimental data available. Swisdak estimated his surface explosion results are accurate to within 15% (Ref. 1), and the underwater explosion data from Cole (Ref. 2) should be at least equally reliable. It should also be pointed out that no component-specific overpressure or impulse fragility test data are available for the equipment in a nuclear power plant intake structure, introducing considerable new uncertainties into the analysis. This situation would benefit greatly from further analysis and/or some scaled fragility experiments.

ACKNOWLEDGMENTS

This work was supported by the Nuclear Regulatory Commission (NRC) and the Defense Threat Reduction Agency (DTRA).

REFERENCES

1. M. M. SWISDAK, "Explosion Effects and Properties: Part II – Explosion Effects in Water," NSWC/WOL/TR 76-116, Naval Surface Weapons Center, Dahlgren, VA, (February 1978).
2. R. H. COLE, *Underwater Explosions*, Princeton University Press, Princeton, NJ, (1948).
3. M. ENEVA, J. L. STEVENS, B. D. KHRISTOFOROV, J. MURPHY, and V. V. ADUSHKIN, "Analysis of Russian Hydroacoustic Data for CTBT Monitoring," *Pure and Applied Geophysics*, 158, pp. 605–626, (2001).
4. M. ENEVA, J. L. STEVENS, J. MURPHY, B. D. KHRISTOFOROV, and V. V. ADUSHKIN, "Analysis of Russian Hydroacoustic Data for CTBT Verification," *Proceedings of the 21st Seismic Research Symposium: Technologies for Monitoring the Comprehensive Nuclear-Test Ban Treaty*, Las Vegas, NV, (Sept. 21–24, 1999).
5. M. P. WHITE, et al., *Effects of Impact and Explosion*, Summary Technical Report of Division 2, NDRC, Washington, DC, (1946).
6. R. H. MORRIS, C. D. SULFREDGE, P. W. GRAHAM, and S. C. WOODSON, "Spent Fuel Pool Experiments Test 1: One-Quarter Scale Experiment," SL-97-11, US Army Corps of Engineers Waterways Experiment Station, Vicksburg, MS, (September 1997).
7. C. S. ROBINSON, *Explosions, Their Anatomy and Destructiveness*, McGraw-Hill, New York, NY, (1944).